

Article

Spatiotemporal Characterization of Chromophoric Dissolved Organic Matter (CDOM) and CDOM-DOC Relationships for Highly-Polluted River

Sijia Li ^{1,2}, Jiquan Zhang ^{1,*}, Guangyi Mu ^{2,3}, Hanyu Ju ¹, Rui Wang ¹ and Danjun Li ¹

¹ Nature Disaster Research Institute, Environment College, Northeast Normal University, Changchun 130024, China; lisj983@nenu.edu.cn (S.L.); juhy287@nenu.edu.cn (H.J.)

² Key Laboratory of Wetland Ecology and Environment, Northeast Institute of Geography and Agroecology, China Academic Science, Changchun 130102, China

³ Grassland Science Institute, Life Science College, Northeast Normal University, Changchun 130024, China

* Correspondence: zhangjq022@nenu.edu.cn; Tel.: +86-135-9608-6467; Fax: +86-431-8916-5624

Abstract: Spectral characteristics of CDOM in water column are a key parameter for bio-optical modeling. Knowledge of CDOM optical properties and spatial discrepancy based on the relationship between water quality and spectral parameters in Yinma River watershed with in situ data collected highly-polluted waters are exhibited in this study. Seasonal field data sets collected over a period of 2 months in 2015 in Yinma River Watershed. Based on the comprehensive index method, the riverine waters showed serious contamination, especially the COD, Fe, Mn, Hg and DO were out of range contamination warning. Dissolved organic carbon (DOC) and total suspended matter (TSM) with prominent non-homogenizing were significantly high in the riverine waters, but chlorophyll-a (Chl-a) was opposite. Ternary phase diagram showed that non-algal particles absorption played an important role in total non-water light absorption (>50%) in most sampling locations, and mean contribution of CDOM were 13% and 22% in summer and autumn respectively. Analysis of ratio of absorption at 250-365 nm ($E_{250:365}$) and spectral slope ($S_{275-295}$) indicated that CDOM had higher aromaticity and molecular weight in autumn than in summer, is consistent with the results of water quality and relative contribution. Redundancy analysis (RDA) indicated that the environmental variables OSM had a strong correlation with CDOM absorption, followed by heavy metal, e.g., Mn, Hg and Cr⁶⁺. However, for the specific UV absorbance ($SUVA_{254}$), the seasonal values showed opposite results compared with the reported literature. The potential reasons were the more UDOM (uncolored Dissolved Organic Matter) from human source (wastewater effluent) existed in waters. Terrigenous inputs simultaneously are in relation to the $a_{CDOM}(440)$ -DOC relationship with the correlation coefficient was 0.90 in summer (2-tailed, $p<0.01$), and 0.58 in autumn (2-tailed, $p<0.05$). Spatial distribution of CDOM parameters exhibited that the downstream regions focused on dry land have high CDOM molecular weight and aromatic hydrocarbon. Partial sampling locations around the cities or countries generally showed abnormal values due to terrigenous inputs. As a bio-optical model parameter, spectral characteristic of CDOM is helpful in adjusting the derived algorithms in highly-polluted environments. The study on organic carbon and pollutants in highly-polluted waters had an important contribution to global carbon balance estimation and water environment protection.

Keywords: chromophoric dissolved organic matter; polluted waters; optical properties; Yinma River watershed

1. Introduction

Chromophoric dissolved organic matter (CDOM), is compositionally complex, representing the optically active fraction of dissolved organic matter (DOM) in natural waters [1-5]. The sources of CDOM in aquatic ecosystem include two parts: autochthonal (microbial and phytoplankton) and allochthonous sources (terrestrial and anthropogenic inputs) [1, 6-8]. Simultaneously, the major sink of CDOM in natural waters is by photo-chemical degradation and microbial consumption processes, and release nutrients to sustain the growth of phytoplankton and bacteria [9-10]. In these biological processes, CDOM could release biologically labile compounds (e.g., the hydroxyl sulfide) and greenhouse gases (CO_2 and CH_4), which could contribute to global warming [11-14]. Absorption characteristic of CDOM in the visible band has been shown to interfere with satellite water color estimates of phytoplankton chlorophyll in aquatic systems [15-16]. Conversely, CDOM is potentially estimated by remote sensing technology with the advantages of time-saving and low-cost. Hence, the ability to quantify and differentiate sources of CDOM in aquatic environments is important for the understanding of biogeochemical carbon cycles, ecosystem integrity, and water quality management.

Remotely sensed imagery, spatial technologies and computer processing are increasingly useful in monitoring of CDOM in recent decades [16-17]. In addition, various studies demonstrated that there existed a positive correlation relationship between the CDOM and dissolved organic carbon (DOC), and CDOM can be used as an inexpensive and rapid proxy for DOC in aquatic environment [18-19]. Estimated CDOM values could be converted into DOC concentration using the regression models [20]. Owing to the regional differences of organic carbon content in near-surface soils, the composition of DOM in aquatic environment is highly heterogeneous, and the relationship between CDOM and DOC is not a constant based on field observations [21-23]. DOC concentrations in arctic rivers, e.g., Kolyma River, are markedly higher during the spring freshet, and lower and more stable through time from July-October [24-25]. Particularly, the composition, properties and distribution of DOM/CDOM in riverine waters showed the more uncertainties threaten by the changes of hydrology, geomorphology, land use/cover, soil types, and seasonality meteorology. CDOM properties are influenced by changed physical, chemical and biological processes which contribute to formation, transformation and degradation. In addition, DOM/CDOM composition changed rapidly in highly dynamic periods (storms and spring freshets), e.g., for the arctic waters, DOC concentration during the spring freshet and summer discharge are markedly higher, but lower in autumn [20, 26]. Hence, compared with the oceanic waters, the allochthonous source is proposed as a critical factor to determine the spatio-temporal variations of CDOM in riverine waters.

Domestic and industrial sewage discharge has resulted in serious organic pollution in many riverine environments. In particular, fecal substances may contain many pathogenic microorganisms are hazardous to human health [19]. CDOM absorption characteristic and fluorescence could serve as a good indicator of contamination and a surrogate for the DOC, biochemical oxygen demand (BOD), chemical oxygen demand (COD) and heavy metal [27-29]. DOM and specifically its CDOM including humic-like and proteinous substances may form water-soluble complexes with multiple organic and inorganic pollutants, thus, enhance their release from the sediments and their mobility. The volatility of pollutants, bio-availability, toxicity and

photo-degradation may be affected by interactions with CDOM. Many studies on CDOM characteristic focused on the riverine waters recently [30-32]. For the highly-polluted waters, it needs to be better quantified to understand the potential impacts of allochthonous source on riverine carbon cycle in spatio-temporal scales and supplement water carbon-cycle database. Optical measurements could constitute a potentially viable approach to detect anomalous changes in water quality [19, 33] (Stedmon et al., 2011; Bieroza et al., 2009). The photo-degradation of CDOM generally results in the loss of CDOM absorption and increases the spectral slope ($S_{275-295}$) [34].

Songhua River is the seventh biggest rivers in China, and the second Songhua River and Nenjiang River are the important tributaries. The first heavy industrial base in China was established in the Songhua watershed, and the major grain producing areas. Machine building industry, chemical industry, power and manufacturing, logging industry, metallurgical industry, textile industry and grain processing industry are widely dispersed in this watershed. Water consumption of agriculture, industry and daily living are come from the main tributaries. In these processes, domestic and industrial sewage and return water of farmland irrigation are discharged into the rivers. The accumulation of heavy metals in sediments and bio-accumulation of benthic organisms were highlighted for Songhua fluvial system recently. Previous studies showed that there are 480 pollutants in the Songhua River, and the main pollutants are COD, phenols, and ammonia nitrogen, etc [35]. The government of Heilongjiang Province had strengthened pollution management, and the water quality pollution can be controlled. However, water quality of several tributaries still showed the serious pollution, as the Yinma River and Yitong River supplies large amounts of organic matter to the Songhua fluvial system. These rivers flow through the Shitoukoumen Reservoir and Xinlicheng Reservoir which are the drinking water source of Changchun City. It is a global problem that safety of drinking water in the drinking water sources [36]. Quantitative estimation and monitor of CDOM in highly-polluted riverine environments give an early warning of contamination of the drinking water supply [19]. It holds a great potential to estimate DOC concentration and organic pollutants via CDOM in the surface layer. In this study, water samples were collected in Yinma River watershed from August to October 2015. CDOM absorption spectrum, relative contribution, absorption coefficients and spectral slope are used to examine compositional distribution and sources, and build linkages to DOC concentration in the Yinma River watershed. *In situ* data sets could also be used for further improvement of the accuracy of algorithms for highly-polluted waters. Environmental factors effected the spectrum of CDOM was selected to illustrate the potential of absorption spectroscopy as a monitoring tool for organic pollutants in highly-polluted riverine waters.

2 Materials and Methods

2.1 Study Area

The Yinma River Watershed (124°58'~126°24'E, 43°02'~44°53'N), an important tributary of Songhua fluvial system, located in central of Jilin province China (Fig.1). The area of watershed is about 1.74×10^4 km², including two main rivers as Yinma River and Yitong River. The region is a typical North temperate zone continental monsoon climate, with a frozen period about 150 days. It has distinct seasons with a windy spring, a hot and rainy summer, a large temperature difference autumn, and a cold dry winter. The mean annual temperature is 5.3°C, yearly average precipitation

ranges from 370 to 668 mm and evaporation is 1438.4 mm. Yinma River originated in the southeast of Yitong Country, and it merges with Yitong River in Nong'an Country and flows to the Second Songhua fluvial system. East of the watershed is the transition zone between mountain and Songliao Plain; Southern is a continuous foothill; northwest is Songliao Plain. The main tributaries of watershed include Wukai River, Chalu River and ShuangYang River. The plain areas account for 60%, and other 40% are the mountain.

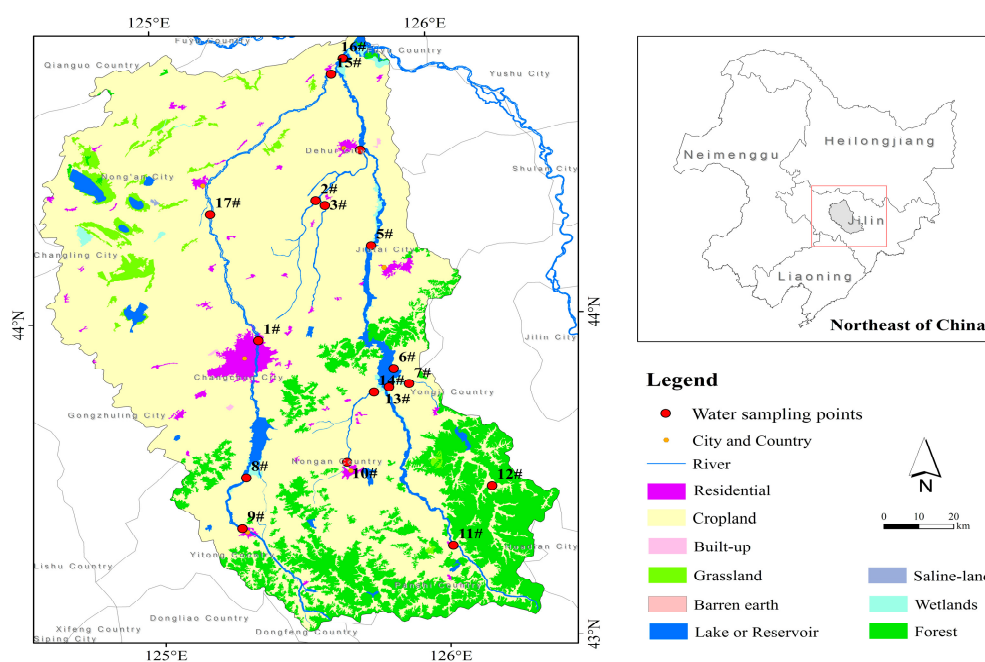


Figure 1. Location and sampling locations of study area, including Yitong River (YT, 5 sampling locations), Yinma River (YM, 11 sampling locations) and 16# in the confluence of the Yinma and Yitong Rivers. The spatial distribution of sampling locations and CDOM-related parameters were determined with ArcGIS 10.1.

2.2 In situ data collection and processing

River plume samples were collected from a sample grid developed for the National Major Program of Water Pollution Control and Treatment Technology of China. Water samples at 17 sites in the watershed were taken from the surface layer (0-0.2 m) during 19th to 22th in August and 29th to 30th in October 2015 (Fig.1). Coordinates for water sample sites were recorded using a global positional system (G350, UniSreong, China); Temperature was measured by thermometer. It's notable that the Perspex water sampler and Niskin bottles were rinsed before collecting by Milli-Q water, and then were rinsed by water samples. Each sample was collected approximately 2.5 L at each site and immediately analyzed on board or stored at 4°C in the dark, in acid cleaned, pre-combusted amber bottles for laboratory analysis (which belongs to Environment Institute, Northeast Normal University). Physical and chemical parameters, e.g., Chlorophyll-a (Chl-a), DOC concentration, total suspended matter (TSM) as well as particulate and CDOM absorption were determined within 6 h. The pH was measured using a PHS-3C pH meter at room temperature (20±2 °C) in the laboratory.

2.3 Measurement of absorbance and processing

According to the quantitative filter technique (QFT, quantitative membrane filter technique), all the samples were filtered under low vacuum, first through a precombusted Whatman GF/F (1825-047) filter (0.7 μm), then through a prerinsed 25mm Millipore membrane cellulose filter (0.22 μm) into glass bottles. Absorbances of the filtrate was measured between 200 nm and 800 nm at 1 nm interval using a Shimadzu UV-2600 spectrophotometer with Milli-Q water as a reference. Scan settings for the spectrophotometer are as follows: 4 nm slit width, 250-800 nm wavelength range, 1 nm data interval, and 100 nm^{-1} scan rate. The absorption coefficient (a_{CDOM}) was calculated from the measured water optical density (OD) following the Eq. (1).

$$a_{\text{CDOM}}(\lambda') = 2.303 \cdot OD_{\lambda} / L \quad (1)$$

Where $a_{\text{CDOM}}(\lambda')$ is the uncorrected CDOM absorption coefficient at given λ , $OD(\lambda)$ is the optical density at the same wavelength, and L is the cuvette path length in meters. In order to eliminate the internal backscattering, the absorbance at 700 nm was used to correct absorption coefficients [37]. $OD_{(\text{null})}$ is the average optical density over 740-750 nm where the absorbance of CDOM can be assumed to be zero [38].

To determine the absorbance of non-algal particles and phytoplankton were filtered under low vacuum through a precombusted Whatman GF/F (1825-047) filter (0.7 μm), and then measured between 400 nm and 700 nm using a Shimadzu UV-2600 spectrophotometer with blank filter as a reference. The absorbances of non-algal particles were bleached by 0.1% sodium hypochlorite. The absorbances of phytoplankton were calculated from the total particulate subtract from non-algal particles. Absorbance were then converted to the absorption coefficient for total particulate, $a(\lambda)$; non-algal particles, $a_{\text{d}}(\lambda)$; phytoplankton, $a_{\text{ph}}(\lambda)$, and CDOM, $a_{\text{CDOM}}(\lambda)$. The total absorption coefficient is the sum of $a_{\text{d}}(\lambda)$, $a_{\text{ph}}(\lambda)$, $a_{\text{CDOM}}(\lambda)$ and $a_{\text{w}}(\lambda)$, where $a_{\text{w}}(\lambda)$ represents a pure water absorption derived from Smiths et al.(1981) [39].

2.4 Water quality measurement and evaluation

In order to prevent pigments denaturalization, water samples were immediately filtered under low vacuum. Water sampling locations for chlorophyll-a extraction were passed through 0.45 μm fiber, after which chlorophyll-a was extracted with 90% acetone for 48 hours under subdued light conditions. The concentrations were determined with a UV spectrophotometer (Shimadzu, UV-2006 PC) by detailed in Song et al (2012) [39]. TSM, inorganic suspended matter (ISM) and organic suspended matter (OSM) were determined by gravimetrical analysis; and more detailed descriptions of measuring absorption coefficients could be found in Song et al (2012) [38]. It noted that the filters need to remove organic matter on muffle before these processes. Dissolved organic carbon (DOC) sampling locations were acidified with concentrated HCl (100 μL of 2N) to a pH of 2 to remove inorganic carbon until analyzed on a total organic carbon analyzer (Shimadzu, TOC-VCPN) by high-temperature catalytic oxidation (680 $^{\circ}\text{C}$). Potassium hydrogen phthalate was used as a reference. DOC concentration was calculated by subtracting dissolved inorganic carbon (DIC) from total dissolved carbon (TDC). More details can be found in Song et al (2012) [38]. The reproducibility of the analytic procedure was within 2-3% for the current study. Reference to environmental quality standards for surface water (GB3838-2002, China), dissolved oxygen (DO)

was measured by iodometry; chemical oxygen demand (COD) was by dichromate; ammonia nitrogen ($\text{NH}_3\text{-N}$) was by Nessler's reagent colorimetry; iron (Fe) was by flame atomic absorption spectrometry; manganese (Mn) was by Potassium periodate spectrophotometric; zinc (Zn) was by atomic absorption spectrometry; mercury (Hg) was by atomic absorption spectrophotometry; Hexavalent chromium (Cr^{6+}) was by diphenylcarbohydrazide spectrophotometric. The comprehensive index method was used to calculate the relative pollution index, and then evaluate pollution status. The formula as following:

$$P_i = \frac{C_i}{C_0} \quad (2)$$

$$P = \frac{1}{m} \sum_{i=1}^m P_i \quad (3)$$

Where C_i is concentration value of i contamination, and C_0 is evaluation standard of i contamination. P_i is the contamination index. The environmental quality standards for surface water (GB3838-2002) were as reference. Results of comprehensive index was shown in Tab.1

Table 1 Water quality classification based on comprehensive pollution index

P	Level
$P < 0.8$	Qualification
$0.8 \leq P \leq 1.0$	Basic qualification
$1.0 < P \leq 2$	Contamination
$P \geq 2$	Serious contamination

2.5 Paramaterization and statistical analysis

The CDOM absorption generally shows negative exponential attenuation along with the increasing of wavelength, and composition of CDOM affects the absorption characteristic along wavelength [34, 40-41]. $a_{\text{CDOM}}(335)$, $a_{\text{CDOM}}(375)$ and $a_{\text{CDOM}}(440)$ were represented as CDOM concentration [7, 42]. Specific UV absorbance (SUVA) values of the sampling locations were calculated by multiplying DOC concentration-normalized UV absorbance at 254 nm by a factor of 100 (i.e., $100 \times \text{SUV}_{254}/\text{DOC}$) [43]. The SUVA_{254} values related to the content of aromatic hydrocarbon in DOM [43]. According to previous studies [32, 43-44], low SUVA_{254} indicated that the autochthonous sources dominated the organic matter content, conversely high SUVA_{254} represent the allochthonous sources with more vascular plant inputs. $E_{250:365}$, related to the content of aromatic hydrocarbon too, can trace the molecular size of DOM [45]. Humic acid (HA) makes up a high proportion of CDOM from terrestrial inputs, as well as fulvic acid (FA) of CDOM from phytoplankton degradation. CDOM spectral slope coefficient S further provided information on the type and source of CDOM. $S_{275-295}$ was calculated using a nonlinear fit of an exponential function to absorption spectrum according to Eq. (2) [37]:

$$a_{\text{CDOM}}(\lambda) = a_{\text{CDOM}}(\lambda_0) \cdot e^{S(\lambda_0 - \lambda)} \quad (4)$$

Where $a_{CDOM}(\lambda)$ is the CDOM absorption at a given wavelength, $a_{CDOM}(\lambda_0)$ is the reference wavelength (440 nm). The effectiveness of S has been demonstrated with CDOM samples from various waters, ranging from DOC-rich wetlands to photo-bleached coastal waters and lakes over high-altitude plateaus [23, 41, 46]. The coefficient of variation (CV) is computed from the filtered mean and standard deviation of values.

3 Results

3.1 Pollution status

Results of comprehensive polluted index were shown in Tab.2 with the environmental quality standards for surface water (GB3838-2002, China) as reference. The comprehensive index P values were 8.11 and 9.03 with serious contamination in summer and autumn respectively (Tab.2). In particular, the COD, Fe, Mn, Hg and DO were out of range contamination warning. The waters in autumn showed the higher level of pollution. Previous studies have exhibited the COD, NH_3-N , TN, and TP accounted for 44.14%, 53.14%, 82.15% and 78% of total pollutants respectively [35]. There existed a large number of farmland with remains of pesticide and fertilizer, household refuse and livestock dung in the Yinma River watershed.

Table 2. The concentration of water quality parameters and comprehensive indexes for riverine waters

Average	pH	DO (mg/L)	NH_3-N (mg/L)	COD (mg/L)	Fe (mg/L)	Mn (mg/L)	Zn (mg/L)	Hg (mg/L)	Cr^{6+} (mg/L)	P
Standards	6~9	2	2.0	40	0.3	0.1	2.0	0.001	0.1	-
Summer	6.79	2.93	0.07	392.16	0.62	0.28	0.06	0.34	0.012	8.11
Autumn	6.08	9.47	0.15	49.37	2.83	0.54	0.13	0	0.002	9.03

3.2 Water quality

3.2.1 Seasonal variation

The TSM, ISM, OSM, DOC and Chl-a concentration with seasonal variability were observed in the Yinma River Watershed. The average TSM concentration in summer ($152.24 \pm 189.9 \text{ mg L}^{-1}$) is higher than in autumn ($38.5 \pm 64.7 \text{ mg L}^{-1}$). Likewise, the average values of ISM and OSM are 144.7 mg L^{-1} and 7.5 mg L^{-1} respectively in summer and 35.3 mg L^{-1} and 3.2 mg L^{-1} in autumn. The high TSM concentration are largely stemmed from allochthonous inputs (Yu et al., 2015), and they are probably associated with soil organic matter [22]. In total, average Chl-a concentration in the summer ($28.3 \pm 57.2 \text{ }\mu\text{g L}^{-1}$) is lower than in autumn ($30.5 \pm 46.2 \text{ }\mu\text{g L}^{-1}$). In addition, the high loads of suspended matter prevent phytoplankton from growing due to light limitation and microbial activity. The high Chl-a concentration observed in the autumn indicated continuous inputs of the wastewater in the watershed, were consistent with the results of comprehensive polluted index. The inputs exceeded the self-purification ability of rivers even in the concentrated rainfall period. The decrease of river discharges was the one of impact factors on low Chl-a concentration in autumn. According to Tranvik et al (2009) [13], 2.9 Pg C yr^{-1} carbons migrate, transforms, and stores via the inland water ecological system. DOC represents an essential link between terrestrial and

aquatic ecosystems [47]. The DOC concentration ranged from 2.4 to 14.4 mg L⁻¹ with the average value was 5.6 mg L⁻¹ in summer, and higher average value was 8.7 mg L⁻¹ in autumn (4.3-19.1 mg L⁻¹).

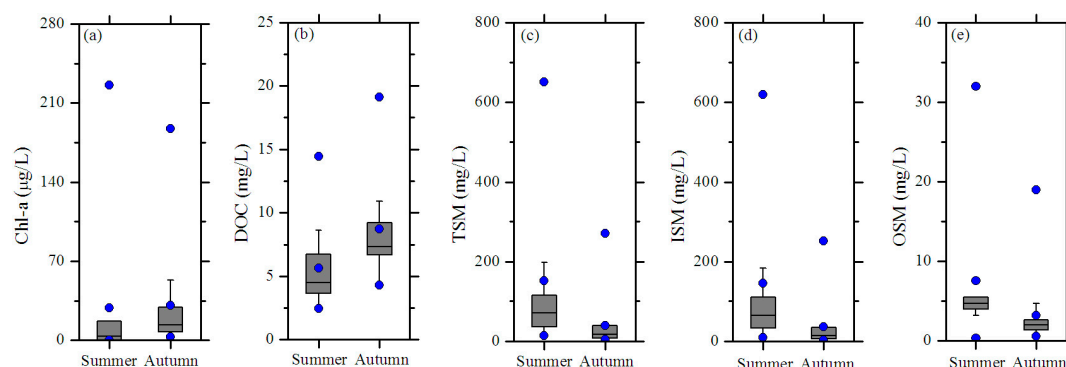


Figure 2. Box plots of dissolved carbon, total suspended matter and chlorophyll-a in the watershed, Yitong River, Yinma River and STKM Reservoir: (a) Chlorophyll-a concentration (µg/L) ($F=0.015$, $p>0.05$), (b) DOC concentration (mg/L) ($F=6.4$, $p<0.05$), (c) Total suspended matter (mg/L) ($F=5.4$, $p<0.05$), (d) Inorganic suspended matter (mg/L) ($F=5.5$, $p<0.05$) and (e) Organic suspended matter ($F=3.7$, $p>0.05$). The horizontal edges of the boxes denote the 25th and 75th percentiles; the whiskers denote the 10th and 90th percentiles and the blue circles represent outliers.

The positive relationships between DOC and NH₃-N were established in summer and autumn ($r=0.78$ and 0.81 ; 2-tailed, $p<0.01$). It is a pity that we have not measured the TN and TP in the surface waters in summer. Regression analyses were also conducted, and a linear relationship between TN and DOC concentration was shown based on the collected data in autumn (Fig3, $r=0.68$; 2-tailed, $p<0.01$). Jiang et al (2014) found that a correlation relationship between TN and DOC was also shown during rainfall in agricultural and forested wetlands in the Shibetsu watershed, Japan. The relationship between DOM and TN may be used to track the plant-derived source fraction [31].

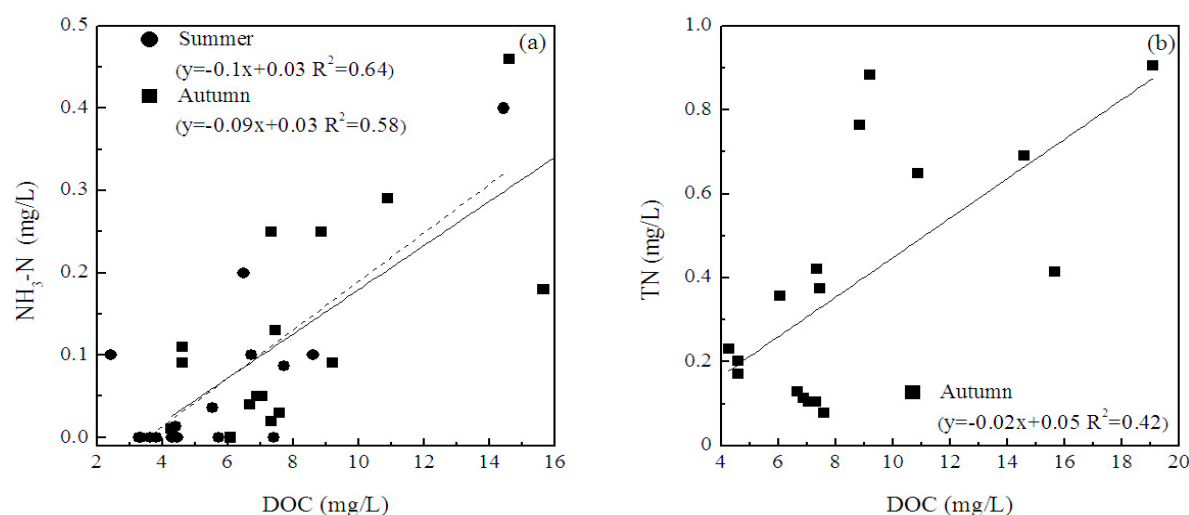


Figure 3. Regression correlation of NH₃-N, TN and DOC for the riverine waters: (a) DOC and NH₃-N in summer and autumn (b) DOC and TN in autumn.

3.2.2 Spatial variation

As shown in Fig.4, the water quality parameters in most of sampling locations were lower than the average values, indicating prominent spatial heterogeneity. NO.1 located in Changchun City possessed the highest Chl-a concentration (225.98 µg L⁻¹) in summer, and there appeared many floated algae like green ribbon floating on the surface of the river during the sampling period. In

the cropland, high Chl-a concentration (e.g. NO.15 and NO.17 in the downstream region of watershed) were exhibited in rivers due to the fertilizer pollution from soil. Chl-a concentration in NO.5 was zero in summer, progressively increasing to the highest value ($187.58 \mu\text{g L}^{-1}$) in autumn. NO.4 and NO.5 around Jiutai City and Dehui City were both higher in autumn (Fig.1). Chl-a concentration in NO.15, NO.16 and NO.17 were relatively high in summer due to accumulation of nutrients from these sampling locations locating in the downstream region.

TSM, OSM and ISM concentration showed the consistent trend in different sampling locations (Fig.4), and ISM occupied the majority of the TSM concentration. NO.9 and NO.12 locating in the upstream region exhibited high values 651.3 mg L^{-1} and 104.67 mg L^{-1} respectively in summer and autumn. TSM concentration in NO.1, NO.8, NO.9 and NO.10 showed the opposite results with DOC and Chl-a concentration, and the high loads of suspended matter prevented phytoplankton from growing due to light limitation. Simultaneously, the surface runoff carried a lot of nutrients could promote the growth of phytoplankton and improve the standing stock of suspended matter.

NO.1 in Yitong River presented the highest DOC (14.44 mg L^{-1}) in summer, and DOC concentration in NO.15 was 19.1 mg L^{-1} in autumn. Seasonal variation of DOC in NO.1, NO.2, NO.3, NO.15, NO.16 and NO.17 locating in downstream region were higher than the average value (7.17 mg L^{-1}). The possible reasons DOM along with other nutrients come from urban and agriculture sewage, and accumulated due to the lower microbial activity. Jiang et al (2014) [48] found that DOC levels in rivers are linked to climate and watershed landscape characteristic.

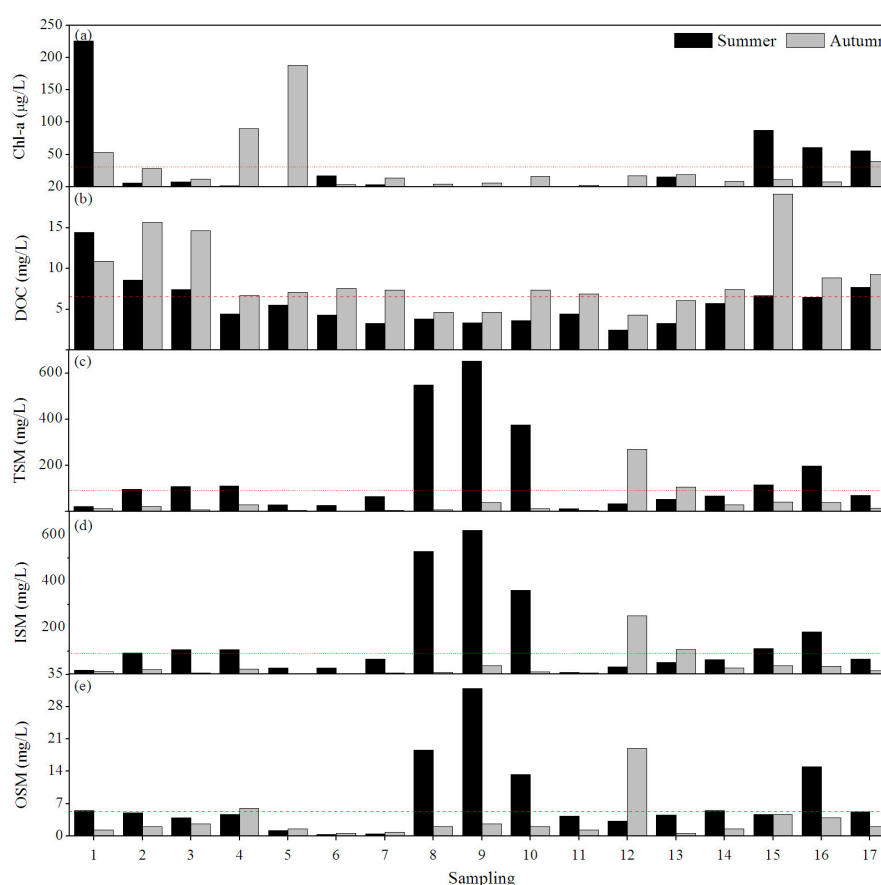


Figure 4. The histogram of DOC, Chl-a, TSM, ISM and OSM concentration in different sampling locations: (a) Chl-a, (b) DOC, (c) TSM, (d) ISM and (e) OSM. The red dash dot lines represent the average values in all the sampling locations.

3.3 Spectral characteristics of CDOM absorption

3.3.1 Seasonal variation

CDOM absorption spectra typically decreases in an approximately exponential fashion with increasing from ultraviolet (UV) to visible wavelengths (Fig.5), similar to CDOM samples from various natural environments [49]. It indicated that the presence of complex optical active constituents over all the sampling locations collected in Yinma River watershed. Noting that high standard deviations for these values reached ~50% indicated high spatio-temporal variability in a_{CDOM} (Fig.5). CDOM absorption coefficient at specific wavelength has often been used as a surrogate for colored DOM [50-51]. The average $a_{\text{CDOM}}(335)$, $a_{\text{CDOM}}(375)$ and $a_{\text{CDOM}}(440)$ in autumn have exhibited significantly higher CDOM light absorption than in summer (Tab.3), were consistent with the changes of water quality (DOC and Chl-a). The use of spectral slopes ($S_{275-295}$) and absorption ratio ($E_{250:365}$) for the tracking of changes in CDOM molecule size has been practically conducted to calculated as indicators [41]. As shown in Tab.3, increasing $E_{250:365}$ values indicated a decrease in aromaticity and molecular weight of CDOM, and higher average $E_{250:365}$ (11.7 ± 11.5) were observed in summer than in autumn (6.4 ± 2.8). It demonstrated relatively high molecular weight CDOM and aromaticity in the rivers in autumn. Recently, a large number of field and laboratory studies have proven that S values were inversely proportional to molecular weight of CDOM, with steeper spectral slope signifying a decreasing of aromaticity, and a shallower spectral slope signifying an increasing aromatic content [52]. Concurrently, $S_{275-295}$ could be used as an indicator for terrigenous DOC percentage [53]. $S_{275-295}$ value was $0.0089 \pm 0.0020 \text{ nm}^{-1}$ in summer and $0.0082 \pm 0.0016 \text{ nm}^{-1}$ in autumn (Tab.3). The riverine waters showed higher $S_{275-295}$ than in coastal or oceanic waters, as has been found in other studies undertaken in lakes [16, 31]. Higher $S_{275-295}$ values ($0.0089 \text{ nm}^{-1} \pm 0.0020$) in summer indicated that the decrease of aromatic compounds and the percentage of low molecular weight fulvic acid in CDOM in summer were greater than in autumn.

As an effective index to characterize the DOC concentration, SUVA_{254} values have been proven to have a correlation with DOM aromaticity as determined by ^{13}C -NMR [43]. The SUVA_{254} measurements ($2.3 \pm 0.8 \text{ mg C}^{-1} \text{ m}^{-1}$) in autumn in this environment were lower than in summer ($4.0 \pm 1.4 \text{ L mg C}^{-1} \text{ m}^{-1}$). From the conclusions and conjecture of some studies on SUVA_{254} and hydrophobic organic acid fraction [43-44], higher SUVA_{254} values indicated that the aquatic systems with abundant vascular plant input, and the allochthonous sources dominated the organic matter content. Conversely, the lower values showed more autochthonous sources (algal and microbial). According to the Fig.2 and Fig.5(b), the smaller seasonal disparities at 254 nm of CDOM absorption and larger in DOC concentration may be responsible for the cause by higher SUVA_{254} in summer, which the ratio of SUVA_{254} is $a_{\text{CDOM}}(254)/\text{DOC}$. Although our study found the inverse results for high polluted waters, the potential reasons may be the more UDOM (Uncolored Dissolved Organic Matter, UDOM) existed in the riverine waters [54].

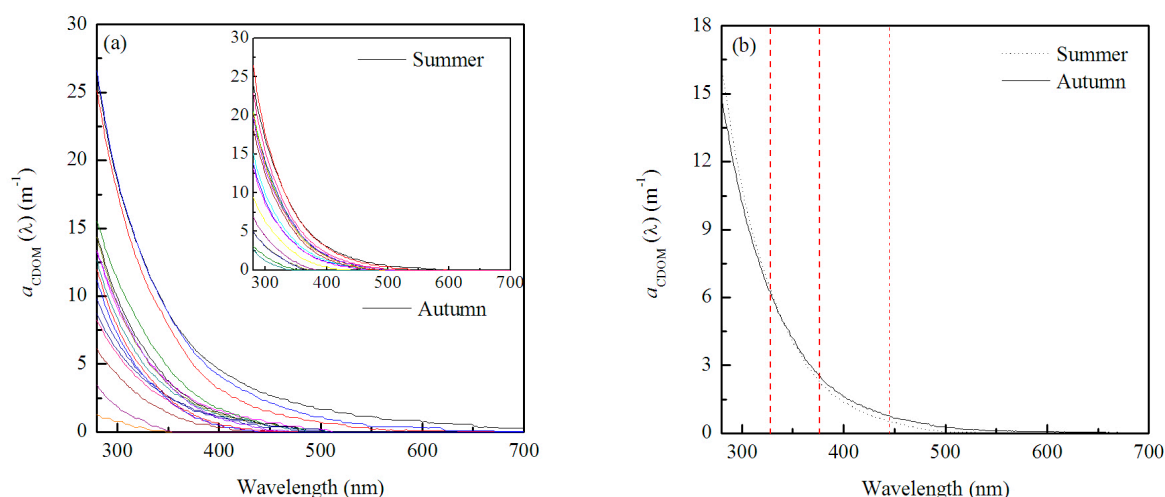


Figure 5. Absorption characteristics of sampling locations from the Yinma watershed : (a) absorption spectrums of CDOM (a_{CDOM}), (b) average absorption spectrums of CDOM (a_{CDOM}). The red line marks at 335, 375 and 440 nm.

Table 3. CDOM absorption parameters of water sampling locations collected in the watershed

	Summer		Autumn	
	Avg \pm SD.	Min-Max	Avg \pm SD.	Min-Max
$a_{\text{CDOM}}(335)$	5.5 ± 3.5	0.3 - 10.6	5.4 ± 3.5	0.3 - 12.3
$a_{\text{CDOM}}(375)$	2.3 ± 1.8	0 - 5.2	2.6 ± 2.0	0 - 6.9
$a_{\text{CDOM}}(440)$	0.6 ± 0.6	0 - 1.7	0.8 ± 0.9	0 - 3.1
SUVA ₂₅₄	4.0 ± 1.4	1.6 - 6.3	2.3 ± 0.8	0.6 - 3.5
$E_{250:365}$	11.7 ± 11.5	0 - 38.7	6.4 ± 2.8	0 - 10.1
S ₂₇₅₋₂₉₅	0.0089 ± 0.0020	0.0069 - 0.0147	0.0082 ± 0.0016	0.0066 - 0.0123

Units of the absorption coefficients of CDOM are m^{-1} , S₂₇₅₋₂₉₅ is nm^{-1} and the unit SUVA₂₅₄ is $\text{L mg}^{-1} \text{C}^{-1} \text{m}^{-1}$.

3.3.2 Spatial variation

Sampling locations were collected at every station from 1# to 17# to achieve better resolution of spatial variability (Fig.6). Seasonal $a_{\text{CDOM}}(335)$, $a_{\text{CDOM}}(375)$ and $a_{\text{CDOM}}(440)$ of NO.12 and NO.13 locating in the upstream region were relatively lower than the sampling locations in the downstream region. Owing to the inputs of urban sewage, NO.10 locating around Shuangyang Country showed high CDOM. Many loads of sewage accumulated in the downstream, resulting in the relative high CDOM found in NO.15, NO.16 and NO.17. Seasonal $E_{250:365}$ showed a polarization phenomenon in different sampling locations (Fig.6). Following the recommendations of recent studies, the relatively high $E_{250:365}$ values in NO.8, NO.9 and NO.10 with low content of aromatic hydrocarbon and molecule weight were remarkable in summer. However, there not existed significant spatial disparities in autumn (Fig.6), and the cause by the phenomenon in autumn may be the reduced run-off and precipitation. Due to the seasonal $a_{\text{CDOM}}(365)$ values were zero values, low $E_{250:365}$ values were observed in NO.12 and NO.13, which the ratio of $E_{250:365}$ is

$a_{\text{CDOM}}(250)/a_{\text{CDOM}}(365)$. However, high $S_{275-295}$ values were observed in NO.12 and NO.13 (Fig.6), signifying a decrease in aromaticity and molecular weight of CDOM.

Relatively lower SUVA_{254} measurements were found in the upstream region (NO.8, NO.9, NO.10, NO.12, and NO.13) indicated that the aromatic moieties of CDOM in this environment were lower compared within downstream region in summer. It revealed that the greater contribution of vascular plant matter to DOM and higher molecular weight DOM in the upstream than in the downstream. In summer, the highest SUVA_{254} measurement was found in NO.11 locating in the low mountains and hills and far away from the cities. The $a_{\text{CDOM}}(254)$ and DOC concentration in NO.11 were 28.02 m^{-1} and 4.46 mg/L with the mean values were 22.71 m^{-1} and 5.62 mg/L respectively, which the ratio of SUVA_{254} is $a_{\text{CDOM}}(254)/\text{DOC}$. According to the Brezonik et al (2015) [55], NO.11 had lower color DOC concentration resulting from algal-derived DOC in the waters. There not existed significant spatial difference in autumn (Fig.6). SUVA_{254} in NO.1 showed the highest value in summer with the higher $a_{\text{CDOM}}(254)$ 37.68 m^{-1} (mean value, 14.44 m^{-1}), indicating the increased aromatic hydrocarbons.

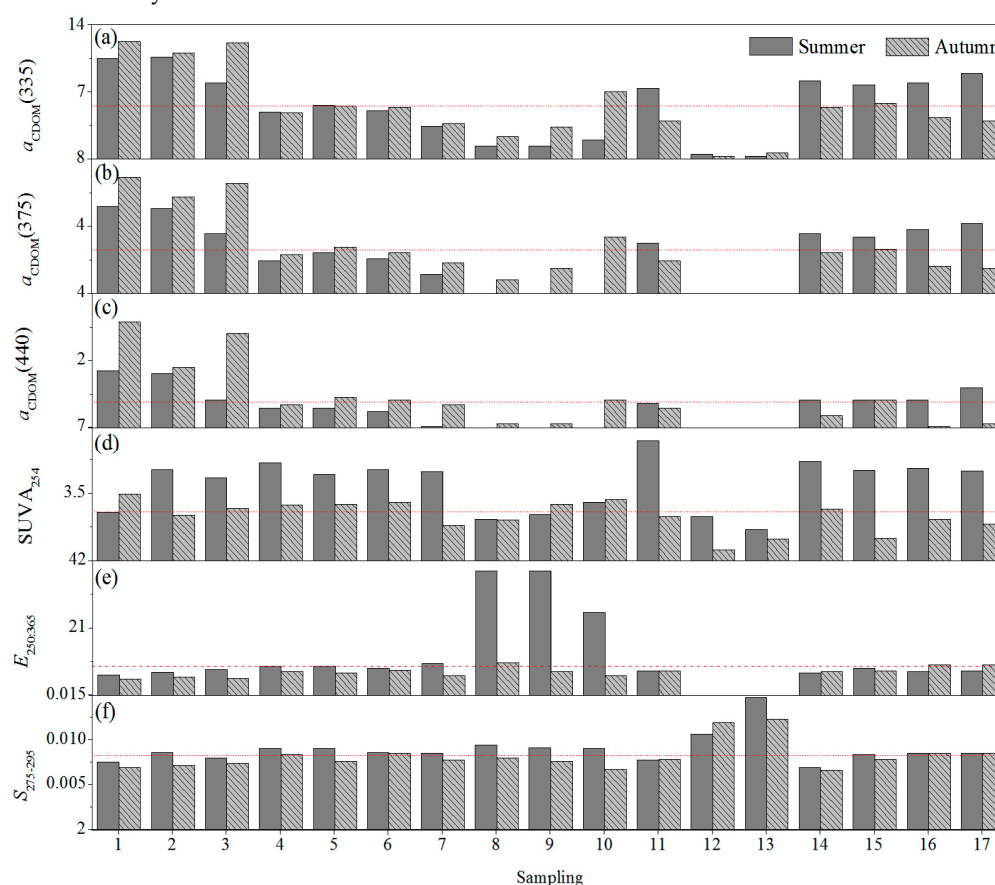


Figure 6. The histogram of $a_{\text{CDOM}}(335)$, $a_{\text{CDOM}}(375)$, $a_{\text{CDOM}}(440)$, SUVA_{254} , $E_{250:365}$ and $S_{275-295}$ in different sampling locations: (a) $a_{\text{CDOM}}(335)$, (b) $a_{\text{CDOM}}(375)$, (c) $a_{\text{CDOM}}(440)$, (d) SUVA_{254} , (e) $E_{250:365}$, (f) $S_{275-295}$. Units of the absorption coefficients of CDOM are m^{-1} , and the unit SUVA_{254} is $\text{L mg C}^{-1} \text{ m}^{-1}$.

3.3 Relative contributions of CDOM absorption

The difference in the contributions of phytoplankton and CDOM to the total absorption could influence the maximum photosynthetic rate and determine the photo-chemical mineralization of DOC [23]. The relative contributions at 440 nm are shown in Fig.7, and there is an obvious seasonal

difference in the relative contributions of CDOM, phytoplankton and non-algal particles. Non-algal particles absorption played a major role on total non-water light absorption in the riverine waters (Fig.7). These reports and the earlier work have suggested that non-algal particles absorption often account for most of the total light absorption for most inland waters [40]. It necessary to classified theses waters according to the variation in optical characteristic in different catchment properties. According to the optical classification of surface waters [56], the waters from Yinma River Watershed both in the summer and autumn could be classified as 'NAP-type'. The mean contribution of CDOM to total contributions is 13% (0~30%) of comparatively minor importance in the summer, and 22 % (0~69%) in the autumn. Relative contribution of non-algal particles and phytoplankton are on mean 78 % (20~100%) and 9% (0~49%) in summer, and 58 % (4~100%), 20% (0~79%) in autumn respectively.

The non-algal particles referring to the TSM occupied a predominant position in the total non-water light absorption (Fig.7). Non-algal particles absorption generally exceeds that of phytoplankton in inland lakes and rivers. TSM concentrations were largely effected by the precipitation, land-cover types and sediment suspension, etc. The second contribution constituent of light absorption was CDOM (Fig.7). As a constituent of DOM, CDOM absorption characteristic is affected by the solar radiation, phytoplankton, microbe activity, river discharge and terrestrial inputs due to the chemical photo-bleaching and microbial degradation, etc. In our opinion, pollutants from the terrestrial inputs were a main factor to responsible for this optical characteristic and high CDOM. For the heavily polluted waters, the relative contributions of optical active constituents to total non-water light absorption showed the wide spatio-temporal variability of DOM loads in riverine ecosystems where numerous and complex physical and biogeochemical factors regulate the interaction between the diverse source and sink process. However, these changes generally related to the local environment factors and climate.

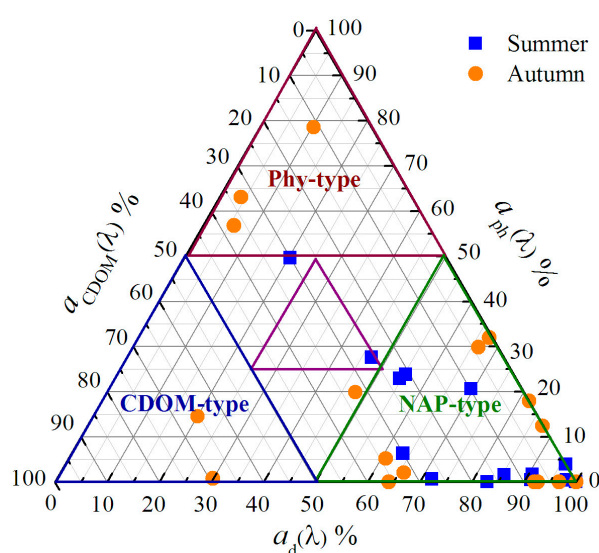


Figure 7. Relative contributions of CDOM, phytoplankton and non-algal particles to total non-water light absorption at 440 nm. According to the optical classification of surface waters (Prieur and Sathyendranath, 1981), the relative contribution of collected water sampling locations could be classified as “CDOM-type”, “non-algal particles type (NAP-type)” and “phytoplankton-type (Phy-type)” due to the variation of water quality parameters.

3.4 Relationship between DOC and CDOM

The presence of significant linear CDOM-DOC relationships have been documented in various coastal, estuaries, lakes and rivers domains in the recent years [32]. Pearson correlation between the CDOM absorption coefficient [$a_{\text{CDOM}}(335)$, $a_{\text{CDOM}}(375)$, $a_{\text{CDOM}}(440)$] and DOC concentration showed that there is a positive correlation between them, and it is possible to calculate the flux of DOC based on CDOM absorption for riverine waters. The correlation coefficient are 0.82, 0.84 and 0.90 in summer (2-tailed, $p < 0.01$), and 0.68, 0.65 and 0.58 in autumn (2-tailed, $p < 0.05$) (Fig.8). These results are in relation to the changes of SUVA_{254} and $a_{\text{CDOM}}(\lambda)$ in different seasons.

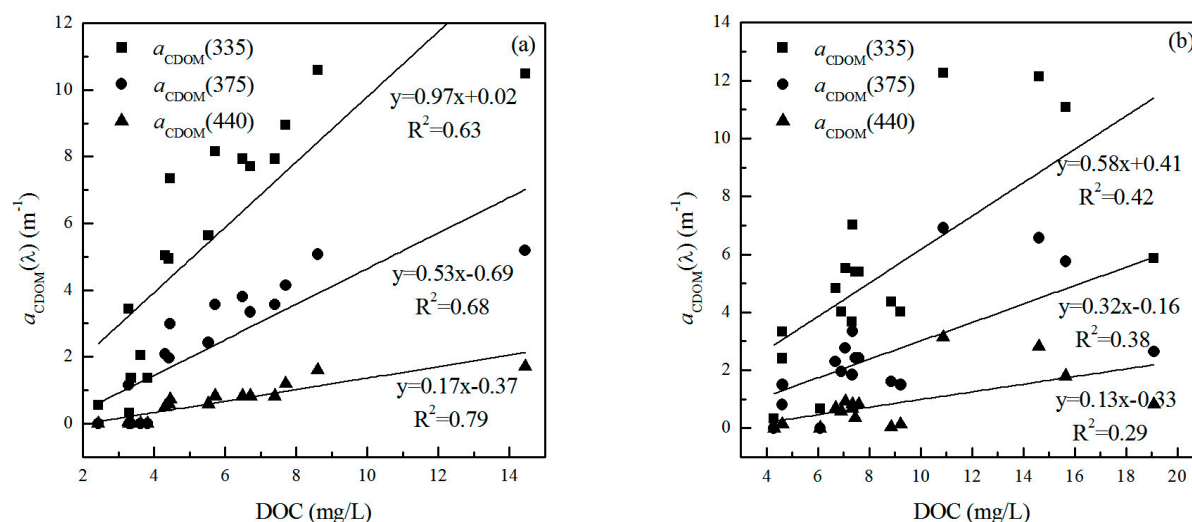


Figure 8. Correlations between $a_{\text{CDOM}}(\lambda)$ and DOC: (a) in summer and (b) in autumn

3.5 Correlations between environmental factors and CDOM absorption

DCA was performed for the response variables in all the sampling locations, and we found that the lengths of gradient were 0.996, 1.320, 1.191 and 1.193 respectively. It demonstrated that the linear relationship between species-environment variables (optical parameters of CDOM and environmental factors) with the values less than 3. In order to achieve the normal distribution data, log-transformed process was performed for the original data before analysis. In addition, there may have a higher correlation among the environmental variables with less contribution. It needs to use RDA to eliminate the invalid environmental variables, e.g., partial correlation coefficient of factors greater than 0.8 and the variance inflation factors greater than 20. Summary of Monte Carlo Permutation Tests were used to testify and validate the variables. The deleted environmental variables mainly contained the TSM, ISM, DOC, Chl-a, pH and $\text{NH}_3\text{-N}$ for the summer sampling locations. Simultaneously, TSM, ISM, DOC, Chl-a, TN, DO, $\text{NH}_3\text{-N}$, COD, Fe, Mn and temperature could be eliminated. These factors generally exhibited high autocorrelation with CDOM.

The relationships between environmental factors and optical characteristic of CDOM were as shown Fig.9. The species-environment correlations were 0.826 and 0.651 in summer and autumn respectively. In summer, the first two axes of RDA could explain 64.2 % (axis 1, 40.4 %; axis, 23.8%) of total variables for the CDOM light absorption. It indicated that COD, Mn and OSM had a strong correlation with CDOM absorption, followed by Hg and Cr^{6+} . Likewise, 36.5% (axis 1, 26.3 %; 10.2 %) was found in autumn. There existed a positive correlation between OSM and CDOM absorption,

followed by Cr^{6+} and TP. CDOM characteristic was effected by the absorb properties of DOM for heavy metal iron. OSM and TP affected the CDOM absorption by the phytoplankton indirectly.

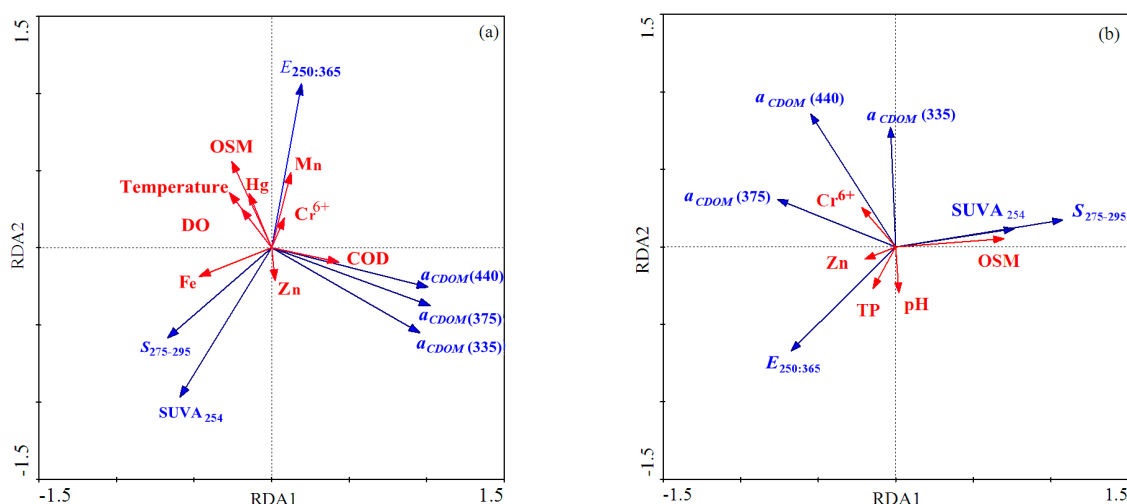


Figure 9. RDA of CDOM absorption and environmental factors:(a) in summer and (b) in autumn

4 Discussion

4.1 Dissolved organic carbon in rivers

DOM, along with other nutrients, derived from soil via runoff and leaching. The high DOC concentration observed in waters indicated the organic-rich nature ecosystem. It was found that grassland and forest always have high nitrogen and organic matter export rates, and the types of land use around the sampling locations may be a crucial factor to the nutrient levels in the waters. Along with the longer residence time, DOC concentration decreases for inland waters in the humid region [32]. Most monitoring data sets indicate that elevated DOC concentration in the semi-arid or arid environment could be related to salinity and attributed to evaporation, potentially due to prolonged water residence times and DOM accumulation [16, 27]. These similar studies were exhibited in terminal waters, e.g., Inner Mongolia Plateau and Hulun Lake [31]. For the heavily-polluted waters (Tab.1), rivers collected waters from many tributaries and streams flow through many cropland and chemical industry in midstream and downstream. The landscape bring more DOM, e.g., polycyclic aromatic hydrocarbon, antibiotic, pesticide and organic pollutants. Human activities are the key factor in determining DOC concentration. In NO.1, it has been shown that there were excessive nutrients when large quantities of domestic and industrial sewage were discharged into watercourses. Under the continuous inputs of the pollutants, concentrated precipitation and river discharge could affect the DOC concentration. Raymond et al (2007) [24] studied the seasonal DOC in high-latitude rivers and found that the DOC is characterized by rising concentration significantly with increasing discharge of rivers. Yinma River watershed located in the semi-arid region, and recharge sources of rivers mainly comes from rainfall. Recently, the Yinma River Watershed has entered dry year, and partial watercourses dried-up due to the precipitation deficit. In particular, for limited rainfall in the autumn, there was only waste water joined in the rivers during the sampling period. River could not purify sewage

based on purification capacities by itself, including reduced pollutant carrying capacity. The DOC results in Yinma River watershed showed the higher value (8.7 mg L^{-1}) in autumn than in summer (5.6 mg L^{-1}). Previous studies [16, 57] showed that the riverine waters have less residence times due to the high lowability and quick exchange rates of flow water enhanced terrestrial DOC inputs, and higher molecular weight humic acid were examined. The positive correlation between the $\text{NH}_3\text{-N}$ and DOC could explain microbial activities and oxidation process between dissolved organic matter and inorganic carbon (Fig.3). Simultaneously, nutritional conditions (TN and TP) had a pronounced influence on the conversion processes through the respiration and reproduction of microbes and phytoplankton [31]. The positive relationship between DOC, $\text{NH}_3\text{-N}$ and TN indicated that an empirical model might be established in polluted waters for estimating DOC storage, with calibration by a comprehensive data set.

4.2 Analysis of CDOM spectral characteristics

In the terminal waters (lakes or reservoirs), high molecular weight CDOM were destroyed by photolysis with the prolongation of hydraulic retention time and irradiation [16, 31]. It found that molecular structure could transform to a low molecular weight pool by the bond cleavage [23]. The UV-photic zone for photo-bleaching in turbid water rarely exceeds 10 cm, so photo-bleaching in these waters is inefficient and mixing masks its effect [42]. In addition, riverine waters have less residence times due to the high lowability and quick exchange rates of flow water and the higher TSM concentration (Fig.2). Non-algal particles absorption played a major role on total non-water light absorption (Fig.7). The synergistic effect of photo-bleaching process is not significant. We suspected the possible conjecture for diverse results in high-polluted waters might be the input of polycyclic aromatic hydrocarbon, pesticide and organic pollutants. In the terrestrially-dominated region, DOC generally varies seasonally in relation to the magnitude of freshwater inputs [59]. This phenomenon implied that the endogenous CDOM pool was probably small relative to the anthropogenic CDOM input to the rivers. In South Atlantic Bight strongly influenced by riverine inflow, water optical properties are determined by high CDOM and sediment input as well as enhanced phytoplankton growth [42]. Precipitation could have a small impact on CDOM optical properties through the river flow indirectly [17, 52]. During low precipitation conditions, $E_{250:365}$ and $S_{275-295}$ in autumn exhibited low values may be caused by fluctuations of river discharge. CDOM characteristic are greatly affected by the precipitation indirectly when the watershed is relative small and the recharge sources of rivers is mainly independent of precipitation. For the large watershed, the influence of precipitation is sporadic. It existed many studies for the SUVA_{254} values in riverine waters, e.g., 30 American rivers (1.31 to $4.56 \text{ L mg C}^{-1} \text{ m}^{-1}$), tropical Epulu River (3.08 to $3.57 \text{ L mg C}^{-1} \text{ m}^{-1}$) and Plateau River (1.08 to $4.79 \text{ L mg C}^{-1} \text{ m}^{-1}$). Although our study found the inverse results for high polluted waters, the potential reasons may be the more UDOM (Uncolored Dissolved Organic Matter, UDOM) existed in the riverine waters (Chen et al., 2004). Further, algal-derived DOC had lower color intensity than DOC from the decomposition of woody vegetation (humic-derived DOC), and DOC from human sources (e.g., wastewater effluent) is nearly uncolored [55]. This is found in the significant CDOM-DOC relationship for riverine waters in summer (Fig.7).

The waters flows the forest showed higher DOC and CDOM than the dry land in the Kolyma river deliver the organic matter to the Arctic Ocean [20]. However, the study on head water streams

draining agricultural and near-pristine catchments (forested and wetland) in the North German plains showed the high DOC in dry land [20]. Compared to other land use types, the dry land make it easier for soil organic matter to the rivers. The use of organic fertilizer in agricultural production could increase organic content matter in the soil. It demonstrated that the downstream waters (NO.15, NO.16 and NO.17) focused on the dry land exhibited the relatively higher CDOM molecular weight and aromatic hydrocarbon. The adverse results of NO.12 and NO.13 were shown in the upstream. The location of garbage and pollutants accumulated sporadically at the downstream of rivers was consistent with areas with concentrated residential areas. Partial sampling locations around the cities or countries generally were abnormal values due to the influence of anthropogenic activities, e.g., NO.10. Along with the continuous inputs of nutrients, decrease of temperature and the low TSM concentration, the relative contributions of phytoplankton to non-light absorption generally increased in sporadic sampling locations (Fig.7). Persistent input of pollutants increased the relative contributions of CDOM absorption in autumn. Industrial proportion achieves the 70% in the Songhua watershed. Agricultural productions also have an important position, and the proportion achieves the 30 %. The point source pollution is a control factor of pollution. In Yinma River Watershed, industrial sectors as Jilin Chemical Industry Corporation and Changchun First Motor Factory are the center of the chemical and machinery. Spatial distribution of CDOM around cities showed the point source pollution is more serious. Conversely, this study focused on the polluted waters could indirectly indicate the scope of point-source. Zhou et al. (2016) [29] used the optimal wavelength derived from CDOM fluorescence as an indicator of point-source contamination in drinking waters, combination of field campaigns in Lake Qiandao and a laboratory waste-water addition experiment. Simultaneously, many sewage plants are only established in Jiutai City and Dehui City, and sewage treatment capacity is insufficient.

4.3 CDOM-DOC relationship and environmental factors

Closer CDOM-DOC analysis indicates that it could use CDOM values (whether measured or computed from remote sensing data) to predict DOC concentrations. Spencer et al. (2012) [32] recently concluded from a study of 30 rivers, that CDOM could be used as a surrogate for DOC in most major rivers of North America. Previous studies have focused on the variability with different r^2 values for CDOM-DOC relationships [59]. The best-fit relationships were linear and involved log transformations. The correlation coefficients were found more significant in summer than in autumn with the DOC concentration ranged from 2.4 to 19.1 mg/L (Fig.9). The major cause of this variability likely is hydrologic variations in the contributing watershed (e.g., variable input of runoff containing colored humic material from forests and wetlands). The fraction of easily degradable riverine DOM that was not included in the CDOM was estimated to be between 8 and 26% of the overall DOC [60].

Stanely et al., (2012) [61] found that human activities such as intensive agriculture or input of waste water effluent can have large effects on the nature of DOC in rivers and streams. These results are in relation to the changes of $SUVA_{254}$ and $a_{CDOM}(\lambda)$ in different seasons. When the ratio of CDOM and UDOM or the CDOM to the DOC is constant, the better CDOM-DOC relationship could be found [54]. Brezonik et al. (2015) [55] reported that when data sets are restricted to exclude water bodies with heavy impacts from human activities that yield DOC with low color, tight

CDOM-DOC relationships can be observed. Although the nature and source of the less colored DOC in waters are unknown. The waste water effluents have higher EfOM (effluent organic matter) resulting in lower color per unit of DOC. DOC is the main member of EfOM, accounting for about 86% of COD (Shon et al., 2008) [62]. In addition, the association of dissolved iron with DOC affects its color intensity, and spatial variations in iron concentrations thus can affect CDOM-DOC relationships [14, 55]. According to the Tab.1, COD in riverine waters showed higher values (392.16 mg/L) in summer than in autumn (49.37 mg/L), and opposite results could found in Fe concentration. The variations in dissolved iron concentrations would likely lead to poor DOC-CDOM relationships [55].

5 Conclusion

Yinma River Watershed is an important polluted tributary of Songhua River between the terrigenous and riverine environments that were also optically complex due to elevated amounts of particulate and dissolved constituents. Recently, the riverine waters have been seriously polluted based on the high comprehensive index P both in summer and autumn, and COD, Fe, Mn, Hg and DO are out of range contamination warning. The high DOC concentration observed in waters indicated the organic-rich aquatic ecosystems, especially for the waters in autumn. Low discharge and continuous inputs from tributaries and streams bring more DOM, e.g., polycyclic aromatic hydrocarbon, pesticide and organic pollutants in autumn. Diverse optical characteristic of CDOM were obtained from spectral parameters, e.g., $a_{CDOM}(335, 375 \text{ and } 440 \text{ nm})$, $SUVA_{254}$, $E_{250:365}$ and $S_{275-290}$ in different seasons. The following conclusions were obtained: (1) The higher $E_{250:365}$ and $S_{275-295}$ in summer indicated the decrease of aromatic compounds and the percentage of low molecular weight fulvic acid in CDOM than in autumn, and opposite $SUVA_{254}$ values could be found simultaneously according to other studies [16, 32]. The potential reasons may be the more uncolored and anthropogenic UDOM existed in the riverine waters [55]. The downstream waters focused on the dry land exhibited the relatively higher CDOM molecular weight and aromatic hydrocarbon, and opposite results were shown in the upstream. Partial sampling locations around the cities or countries generally are abnormal values due to terrigenous inputs. (2) The positive linear CDOM-DOC relationship was exhibited in the summer with the low comprehensive index P , and these results are in relation to the changes of $SUVA_{254}$ and $a_{CDOM}(\lambda)$. For the heavily polluted waters, the obvious correlations were found in shorter wavelengths. (3) Environmental variables OSM had a strong correlation with CDOM absorption, followed by heavy metal e.g., Mn, Hg and Cr^{6+} in the Yinma River Watershed. TP and OSM derived from algae could affect the CDOM absorption by the phytoplankton for the heavily polluted waters in autumn. Yinma River Watershed as a typical inland riverine waters, do research on polluted waters is representative of other regions effected by anthropogenic activities. A study of the optical-biochemistry correlation is helpful for the CDOM-related remote sensing data of polluted waters, and evaluating the water quality. However, high loading of complex CDOM inputs from anthropogenic activities, constitutes a challenge for deriving CDOM and DOC flux. In addition, $a_{CDOM}(\lambda)$, as a parameters of bio-optical model, is sensitive to changes in the specific composition of water constituents and may not showed the completely exponential function. For the high polluted waters, many algorithms may show more uncertainties [63]. It needs high spectral resolution of sensors, consecutive observations and improvement of arithmetic.

Acknowledgments

This study was financially supported by the National Major Program of Water Pollution Control and Treatment Technology of China under Grant No. 2014ZX07201-011-002. We thank the editor and the anonymous reviewers for their helpful comments. We thank Wen Zhidan from the Northeast Institute of Geography and Agroecology, China Academic Science, for statistical assistance.

Author Contributions

All authors contributed significantly to this manuscript. Zhang was responsible for the original idea and the theoretical aspects of the paper. Li and Mu were responsible for the data collection and preprocessing, Ju and Wang were responsible for the methodology design, and Li drafted the manuscript and all authors read and revised the final manuscript.

Conflicts of Interest

The authors declare no conflict of interest.

References

1. Coble P G. Characterization of marine and terrestrial DOM in seawater using excitation-emission matrix spectroscopy, *Marine chemistry*. **1996**, 51, 325-346.
2. Gao J, Yang H, Li B. Investigating the Roles of Dissolved Organic Matter on Arsenic Mobilization and Speciation in Environmental Water, *CLEAN–Soil, Air, Water*. **2016**.
3. Guo X J, Li Q, Jiang J Y, Dai B L. Investigating Spectral Characteristics and Spatial Variability of Dissolved Organic Matter Leached from Wetland in Semi-Arid Region to Differentiate Its Sources and Fate, *CLEAN–Soil, Air, Water*. **2014**, 42(8), 1076-1082.
4. Ou H S, Wei C H, Deng Y, Gao N Y. Integrated Principal Component Analysis of Microcystis aeruginosa Dissolved Organic Matter and Assessment of UV - C Pre - Treatment on Cyanobacteria - Containing Water, *CLEAN–Soil, Air, Water*. **2014**, 42(4), 442-448.
5. Wetzel R. G. Limnology: lake and river ecosystems, Gulf Professional Publishing. **2001**.
6. D'Sa E J, Miller R L, Del Castillo C. Bio-optical properties and ocean color algorithms for coastal waters influenced by the Mississippi River during a cold front. *Applied Optics*. **2006**, 45, 7410-7428.
7. D'Sa E J, Goes J I, Gomes H, Mouw C. Absorption and fluorescence properties of chromophoric dissolved organic matter of the eastern Bering Sea in the summer with special reference to the influence of a cold pool, *Biogeosciences*. **2014**, 11, 3225-3244.
8. Liang Y, Xiao X, Du E, Song C, Song C, Zhao Y, Liu X. Chromophoric Dissolved Organic Matter Fluctuation Assessment in an Urban River, *CLEAN–Soil, Air, Water*. **2014**, 43(8), 1128-1135.
9. Coble P G. Marine optical biogeochemistry: the chemistry of ocean color. *Chemical reviews*, **2007**, 107, 402-418.
10. Moran M A, Zepp R G. Invited Review Role of photoreactions in the formation of biologically labile compounds from dissolved organic matter, *Oceanography*. **1997**, 42.
11. Mopper K, Zhou X, Kieber R J, Kieber D J, Sikorski R J, Jones R D. Photochemical degradation of dissolved organic carbon and its impact on the oceanic carbon cycle, *Nature*. **1991**, 353, 60-62.

12. Lapierre J F, Giorgio P A. Geographical and environmental drivers of regional differences in the lake pCO₂ versus DOC relationship across northern landscapes, *Journal of Geophysical Research: Biogeosciences*. **2012**, 117(G3).
13. Tranvik L J, Downing J A, Cotner J B, et al. Lakes and reservoirs as regulators of carbon cycling and climate, *Limnology and Oceanography*. **2009**, 54, 2298-2314.
14. Köhler S J, Kothawala D, Futter M N, Liungman O, Tranvik L. In-lake processes offset increased terrestrial inputs of dissolved organic carbon and color to lakes, *PloS one*. **2013**, 8, e70598.
15. Siegel D A, Maritorea S, Nelson N B, Hansell D A, Lorenzi-Kayser M. Global distribution and dynamics of colored dissolved and detrital organic materials, *Journal of Geophysical Research: Oceans*, **2002**, 107(C12).
16. Song K S, Zang S Y, Zhao Y, Li L, Du J, Zhang N N, Liu L. Spatiotemporal characterization of dissolved carbon for inland waters in semi-humid/semi-arid region, China, *Hydrology and Earth System Sciences*. **2013**, 17, 4269-4281.
17. Zhu W, Yu Q, Tian Y Q, Becker B L, Zheng T, Carrick H J. An assessment of remote sensing algorithms for colored dissolved organic matter in complex freshwater environments, *Remote Sensing of Environment*. **2014**, 140, 766-778.
18. Baker A, Bolton L, Newson M, Spencer R G. Spectrophotometric properties of surface water dissolved organic matter in an afforested upland peat catchment, *Hydrological Processes*. **2008**, 22, 2325-2336.
19. Stedmon C A, Thomas D N, Papadimitriou S, Granskog M A, Dieckmann G S. Using fluorescence to characterize dissolved organic matter in Antarctic sea ice brines, *Journal of Geophysical Research: Biogeosciences (2005-2012)*. **2011**, 116(G3).
20. Griffin C G, Frey K E, Rogan J, Holmes R M. Spatial and inter-annual variability of dissolved organic matter in the Kolyma River, East Siberia, observed using satellite imagery, *Journal of Geophysical Research: Biogeosciences*. **2011**, 116(G3).
21. Spencer R G, Hernes P J, Ruf R, Baker A, Dyda R Y, Stubbins A, Six J. Temporal controls on dissolved organic matter and lignin biogeochemistry in a pristine tropical river, Democratic Republic of Congo, *Journal of Geophysical Research: Biogeosciences*. **2010**, 115(G3).
22. Stedmon C A, Markager S. Resolving the variability in dissolved organic matter fluorescence in a temperate estuary and its catchment using PARAFAC analysis, *Limnology and Oceanography*. **2005**, 50, 686-697.
23. Zhang Y, Zhang E, Yin Y, Van Dijk M A, Feng L, Shi Z, Qin B. Characteristics and sources of chromophoric dissolved organic matter in lakes of the Yungui Plateau, China, differing in trophic state and altitude, *Limnology and Oceanography*. **2010**, 55, 2645-2659.
24. Raymond P A, McClelland J W, Holmes R M, Zhulidov A V, Mull K, Peterson B J, Striegl R G, Aiken G R, Gurtovaya T Y. Flux and age of dissolved organic carbon exported to the Arctic Ocean: A carbon isotopic study of the five largest arctic rivers, *Global Biogeochemical Cycles*. **2007**, 21.
25. Holmes R M, Bromiley P, Devers C E, Holcomb T R, McGuire J B. Management theory applications of prospect theory: Accomplishments, challenges, and opportunities, *Journal of Management*. **2011**, 37, 1069-1107.
26. Holmes R M, McClelland J W, Peterson B J, Tank S E, Bulygina E, Eglinton T I, Gordeev V V, Gurtovaya T Y, Raymond P A, Repeta D J, Staples R, Striegl R G, Zhulidov A V, Zimov S A, Staples R. Seasonal and annual fluxes of nutrients and organic matter from large rivers to the Arctic Ocean and surrounding seas, *Estuaries and Coasts*. **2012**, 35, 369-382.

27. Curtis P J, Adams H E. Dissolved organic matter quantity and quality from freshwater and saltwater lakes in east-central Alberta, *Biogeochemistry*. **1995**, 30, 59-76.
28. Kowalczyk P, Cooper W J, Durako M J, Kahn A E, Gonsior M, Young H. Characterization of dissolved organic matter fluorescence in the South Atlantic Bight with use of PARAFAC model: Relationships between fluorescence and its components, absorption coefficients and organic carbon concentrations, *Marine Chemistry*. **2010**, 118, 22-36.
29. Zhou Y, Jeppesen E, Zhang Y, Shi K, Liu X., Zhu G. Dissolved organic matter fluorescence at wavelength 275/342 nm as a key indicator for detection of point-source contamination in a large Chinese drinking water lake, *Chemosphere*. **2016**, 144, 503-509.
30. Shao T, Song K, Du J, Zhao Y, Ding Z, Guan Y, Zhang B. Seasonal Variations of CDOM Optical Properties in Rivers Across the Liaohe Delta, *Wetlands*. **2015**, 1-12.
31. Wen Z D, Song K S, Zhao Y, Du J, Ma J H. Influence of environmental factors on spectral characteristic of chromophoric dissolved organic matter (CDOM) in Inner Mongolia Plateau, China, *Hydrology and Earth System Sciences*. **2016**, 20, 787-801.
32. Spencer R G, Butler K D, Aiken G R. Dissolved organic carbon and chromophoric dissolved organic matter properties of rivers in the USA, *Journal of Geophysical Research: Biogeosciences (2005-2012)*. **2012**, 117(G3).
33. Bieroza M, Baker A, Bridgeman J. Relating freshwater organic matter fluorescence to organic carbon removal efficiency in drinking water treatment, *Science of the Total Environment*. **2009**, 407, 1765-1774.
34. D'Sa E J, DiMarco S F. Seasonal variability and controls on chromophoric dissolved organic matter in a large river-dominated coastal margin, *Limnology and Oceanography*. **2009**, 54, 2233.
35. Jiao K W, Li F X, Zhou Q X. Spatial distribution and pollution level evaluation of nutrients in the Songhua River Basin, *Journal of Agro-Environment Science*. **2015**, 34, 769-775.
36. Williamson C E, Brenttrup J A, Zhang J, Renwick W H, Hargreaves B R, Knoll L B, Overholt E P, Rose K C. Lakes as sensors in the landscape: optical metrics as scalable sentinel responses to climate change, *Limnology and Oceanography*. **2014**, 59, 840-850.
37. Bricaud A, Morel A, Prieur L. Absorption by dissolved organic matter of the sea (yellow substance) in the UV and visible domains, *Limnology and Oceanography*. **1981**, 26, 43-53.
38. Song K, Li L, Wang Z, Liu D, Zhang B, Xu J, Wang Y. Retrieval of total suspended matter (TSM) and chlorophyll-a (Chl-a) concentration from remote-sensing data for drinking water resources, *Environmental monitoring and assessment*. **2012**, 184, 1449-1470.
39. Smith R C, Baker K S. Optical properties of the clearest natural waters (200-800 nm), *Applied optics*. **1981**, 20, 177-184.
40. Carder K L, Steward R G, Harvey G R, Ortner P B. Marine humic and fulvic acids: Their effects on remote sensing of ocean chlorophyll, *Limnology and oceanography*. **1989**, 34, 68-81.
41. Helms J R, Stubbins A, Ritchie J D, Minor E C, Kieber D J, Mopper K. Absorption spectral slopes and slope ratios as indicators of molecular weight, source, and photobleaching of chromophoric dissolved organic matter, *Limnology and Oceanography*. **2008**, 53, 955.
42. Kowalczyk P, Cooper W J, Whitehead R F, Durako M J, Sheldon W. Characterization of CDOM in an organic-rich river and surrounding coastal ocean in the South Atlantic Bight, *Aquatic Sciences*. **2003**, 65, 384-401.
43. Weishaar J L, Aiken G R, Bergamaschi B A, Fram M S, Fujii R, Mopper K. Evaluation of specific ultraviolet absorbance as an indicator of the chemical composition and reactivity of dissolved organic carbon, *Environmental Science Technology*. **2003**, 37, 4702-4708.

44. Cory R M, McKnight D M, Chin Y P, Miller P, Jaros C L. Chemical characteristics of fulvic acids from Arctic surface waters: Microbial contributions and photochemical transformations, *Journal of Geophysical Research: Biogeosciences* (2005-2012). **2007**, 112.
45. Peuravuori J, Pihlaja K. Molecular size distribution and spectroscopic properties of aquatic humic substances, *Analytica Chimica Acta*. **1997**, 337, 133-149.
46. Zhang Y, Qin B, Zhu G, Zhang L, Yang L. Chromophoric dissolved organic matter (CDOM) absorption characteristics in relation to fluorescence in Lake Taihu, China, a large shallow subtropical lake, *Hydrobiologia*. **2007**, 581, 43-52.
47. Cole J J, Prairie Y T, Caraco N F, McDowell W H, Tranvik L J, Striegl R G, Melack J. Plumbing the global carbon cycle: integrating inland waters into the terrestrial carbon budget, *Ecosystems*. **2007**, 10, 172-185.
48. Jiang R, Hatano R, Zhao Y, Kuramochi K, Hayakawa A, Woli K P, Shimizu M. Factors controlling nitrogen and dissolved organic carbon exports across timescales in two watersheds with different land uses, *Hydrological processes*. **2014**, 28, 5105-5121.
49. Baker A, Lamont-Black J. Fluorescence of dissolved organic matter as a natural tracer of ground water, *Ground water*. **2001**, 39, 745-750.
50. Asmala E, Autio R, Kaartokallio H, Pitkänen L, Stedmon C, Thomas D N. Bioavailability of riverine dissolved organic matter in three Baltic Sea estuaries and the effect of catchment land use, *Biogeosciences*. **2013**, 10, 6969-6986.
51. Fichot C G, Benner R. The spectral slope coefficient of chromophoric dissolved organic matter ($S_{275-295}$) as a tracer of terrigenous dissolved organic carbon in river-influenced ocean margins, *Limnology and Oceanography*. **2012**, 57, 1453-1466.
52. Del Castillo C E, Gilbes F, Coble P G, Müller-Karger F E. On the dispersal of riverine colored dissolved organic matter over the West Florida Shelf, *Limnology and Oceanography*. **2000**, 45, 1425-1432.
53. Gonnelli M, Vestri S, Santinelli C. Chromophoric dissolved organic matter and microbial enzymatic activity. A biophysical approach to understand the marine carbon cycle, *Biophysical chemistry*. **2013**, 182, 79-85.
54. Chen Z, Li Y, Pan J. Distributions of colored dissolved organic matter and dissolved organic carbon in the Pearl River Estuary, China, *Continental Shelf Research*. **2004**, 24, 1845-1856.
55. Brezonik P L, Olmanson L G, Finlay J C, Bauer M E. Factors affecting the measurement of CDOM by remote sensing of optically complex inland waters, *Remote Sensing of Environment*. **2015**, 157, 199-215.
56. Prieur L, Sathyendranath S. An optical classification of coastal and oceanic waters based on the specific spectral absorption curves of phytoplankton pigments, dissolved organic matter, and other particulate materials, *Limnology and Oceanography*. **1981**, 26, 671-689.
57. Organelli E, Bricaud A, Antoine D, Matsuoka A. Seasonal dynamics of light absorption by chromophoric dissolved organic matter (CDOM) in the NW Mediterranean Sea (BOUSSOLE site), *Deep Sea Research Part I: Oceanographic Research Papers*. **2014**, 91, 72-85.
58. Rochelle-Newall E J, Fisher T R. Production of chromophoric dissolved organic matter fluorescence in marine and estuarine environments: an investigation into the role of phytoplankton, *Marine Chemistry*. **2002**, 77, 7-21.
59. Müller R A, Futter M N, Sobek S, Nisell J, Bishop K, Weyhenmeyer G A. Water renewal along the aquatic continuum offsets cumulative retention by lakes: implications for the character of organic carbon in boreal lakes, *Aquatic Sciences*. **2013**, 75, 535-545.

60. Borisover M, Bukhanovsky N, Lapides I, Yariv S. Thermal treatment of organoclays: Effect on the aqueous sorption of nitrobenzene on n-hexadecyltrimethyl ammonium montmorillonite, *Applied Surface Science*. **2010**, 256, 5539-5544.
61. Stanley E H, Powers S M, Lottig N R, Buffam I, Crawford J T. Contemporary changes in dissolved organic carbon (DOC) in human-dominated rivers: is there a role for DOC management?, *Freshwater Biology*. **2012**, 57(s1), 26-42.
62. Shon H K, Vigneswaran S, Kim I S, Cho J, Ngo H H. Fouling of ultrafiltration membrane by effluent organic matter: a detailed characterization using different organic fractions in wastewater, *Journal of Membrane Science*. **2008**, 278, 232-238.
63. Joshi I, D'Sa E J. Seasonal Variation of Colored Dissolved Organic Matter in Barataria Bay, Louisiana, Using Combined Landsat and Field Data, *Remote Sensing*. **2015**, 7, 12478-12502.



© 2016 by the authors; licensee *Preprints*, Basel, Switzerland. This article is an open access article distributed under the terms and conditions of the Creative Commons by Attribution (CC-BY) license (<http://creativecommons.org/licenses/by/4.0/>).